Phenotype and Progression of Retinal Degeneration Associated With Nullizigosity of *ABCA4*

Ana Fakin,[1,2] Anthony G. Robson,[1,2] Kaoru Fujinami,[1,3,4] Anthony T. Moore,[1,2,5] Michel Michaelides,[1,2] John (Pei-Wen) Chiang,[6] Graham E. Holder,[1,2] and Andrew R. Webster[1,2]

[1]UCL Institute of Ophthalmology, London, United Kingdom
[2]Moorfields Eye Hospital, London, United Kingdom
[3]National Institute of Sensory Organs, National Hospital Organization, Tokyo Medical Center, Tokyo, Japan
[4]Department of Ophthalmology, Keio University, School of Medicine, Tokyo, Japan
[5]Department of Ophthalmology, University of California, San Francisco School of Medicine, San Francisco, California, United States
[6]Casey Molecular Diagnostic laboratory, Portland, Oregon, United States

Correspondence: Andrew R. Webster, UCL Institute of Ophthalmology, 11-43 Bath Street, London EC1V 9EL, England; andrew.webster@ucl.ac.uk.

Submitted: April 27, 2016
Accepted: July 8, 2016

Citation: Fakin A, Robson AG, Fujinami K, et al. Phenotype and progression of retinal degeneration associated with nullizigosity of *ABCA4*. *Invest Ophthalmol Vis Sci*. 2016;57:4668–4678. DOI:10.1167/iovs.16-19829

Purpose. We describe the phenotypes associated with nullizigosity and nine splicing mutations in the *ABCA4* gene.

Methods. The study included 19 patients with biallelic null mutations (Group A, nullizygous), 27 with splicing mutations in the homozygous state or in trans with a null mutation (Group B), and 20 with p.G1961E in trans with a null mutation (Group C, control). Ages at onset and visual acuities were determined from medical histories. Area of decreased autofluorescence within a 30° × 30° fundus autofluorescence (FAF) image was measured with the Region Finder ($N = 58$). Full-field electroretinography (ERG) was performed incorporating the International Society for Clinical Electrophysiology of Vision (ISCEV) standard ($N = 40$).

Results. For groups A to C, the median ages of onset were 6, 8, and 17, respectively. Kaplan Meier survival analysis estimated that 50% of patients reached visual acuity below 20/400 at the ages of 29, 48, and 66 years, respectively. The area of reduced FAF was estimated to increase by 1.5, 1.2, and 0.03 mm^2 per year, respectively, and cone–rod dystrophy was present in 10/12, 13/15, and 0/13 of cases, respectively. Splicing mutation c.5714+5G>A was associated with a significantly milder phenotype in comparison with nullizygous patients for all parameters.

Conclusions. Nullizygosity for *ABCA4* is associated with early onset cone–rod dysfunction with rapid progression shown by enlargement of central atrophy on FAF, decline of ERG amplitudes with age, and a high risk of reaching legal blindness by the fourth decade. Most studied splicing mutations were associated with a similarly severe phenotype. Estimated rates of progression may facilitate further genotype–phenotype correlations and inform the design of treatment trials.

Keywords: ABCA4, macular dystrophy, Stargardt dystrophy, fundus autofluorescence, optical coherence tomography

Mutations in the *ABCA4* gene cause more cases of inherited blindness than any other gene, creating a considerable burden on affected patients and families and society as a whole. So far, all reported disease-causing mutations act in a recessive manner and cause a spectrum of phenotypes described with terms, such as Stargardt disease, macular dystrophy, fundus flavimaculatus, cone–rod dystrophy, and retinitis pigmentosa; an all-encompassing term being ABCA4-retinopathy. The disorder has been the subject of much research and trials of novel therapies, including gene replacement and stem cell therapies are underway.[1] Nullizygosity for *ABCA4*, predicted to result in an absence of ABCA4 protein in the retina, has been observed previously to cause severe disease.[2–4] However, to our knowledge, the severity and range of phenotypic variability has not been studied in a large cohort. The main purpose of the present study was to characterize the phenotype and progression rates of biallelic null mutations in *ABCA4*. An additional purpose was to characterize the phenotypes associated with nine different splicing mutations. For comparison, the phenotype associated with hemiziyosity for the most common missense allele, p.Gly1961Glu is described in parallel.

Methods

Patient Selection

Patients were ascertained from a cohort of 424 patients who presented to Moorfields Eye Hospital with findings consistent with ABCA4 retinopathy, in whom genetic analysis had revealed at least two *ABCA4* mutations. The cohort consisted of (Group A) 19 patients with two truncating mutations in *ABCA4* (stop or frame-shifting mutations; 84% male; median age at the last visit, 19 years; range, 6–75), (Group B) 27 patients with either a splicing mutation in trans with a truncating mutation or homozygous for a splicing mutation (52% male; median age at the last visit, 19 years; range, 8–68), and (Group C, control

Investigative Ophthalmology & Visual Science

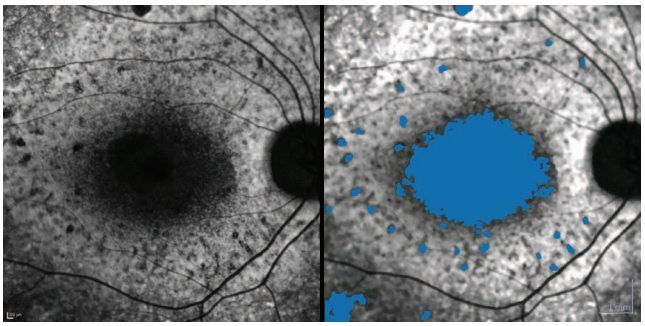

FIGURE 1. Measurement of the total area of decreased autofluorescence within the 30° × 30° FAF image using Region Finder software (the Heidelberg Spectralis Region Finder tool).

group) 20 patients with the most common *ABCA4* mutation, p.G1961E, in trans with a likely-null mutation (truncating or splicing mutation with the exception of c.5714+5G>A; 60% male; median age at the last visit, 36 years; range, 20–70).

Clinical Assessment

Disease onset was defined as the age when patients first reported visual problems. Visual acuity (VA) was determined using Snellen charts and converted to logMAR ($N = 64$). Counting finger and hand motion were quantified as 2.0 and 2.3 logMAR,[5] and light perception as 2.8 logMAR.[6] Kaplan-Meier survival analysis was performed using best corrected VA below 20/400 (6/60 or 1.3 logMAR) as threshold. The better eye was used for the analysis of VA as it was thought to best reflect of the effect of the central visual loss on the patient's daily life. Fundus appearance was classified according to Fishman groups: I – flecks limited to within the vascular arcades, II – fleck-like lesions anterior to the vascular arcades and/or nasal to the optic disc, III – most diffuse flecks resorbed leaving diffuse RPE atrophy, and IV – not only diffusely resorbed fundus flecks and atrophy of the RPE but also diffuse choriocapillaris atrophy.[7]

Fundus Autofluorescence and Optical Coherence Tomography (OCT)

Fundus autofluorescence (FAF) and OCT (Spectralis, Heidelberg, Germany) were performed on at least one occasion in 14, 24 (23 with volume OCT scan), and 20 (17 with volume OCT) patients from groups A to C, respectively, and on two or more occasions in 5, 14, and 17 patients, respectively, with mean follow-up periods between the first and last imaging of 5, 4, and 5 years, respectively. The clinical appearance was usually very symmetrical on both eyes and the right eye was used for measurements, except in cases with poor image quality. The Region Finder tool was used on the 30° × 30° FAF images as described previously.[8] In short, this semiobjective tool, available in the Heidelberg Spectralis software, was used to measure the total area of decreased FAF, similar in intensity to that of the optic disc, presumed to represent dysfunctional and/or absent RPE (example in Fig. 1). Optical coherence tomography was used in some individuals to help differentiate areas of abnormally decreased FAF (associated with loss of outer retina) from normal but dense macular luteal pigment. The results in millimeters squared were converted to degrees squared using the manufacturer's conversion for the average eye (1 $mm^2 = 10.87\ deg^2$). The area of decreased FAF was plotted against age; linear regression, as well as longitudinal analysis was used to estimate the rates of disease progression in the central 30° × 30° area. The 95% confidence interval (CI) of the nullizygous group was used to determine whether the splicing mutations were resulting in a null-like or comparatively milder phenotype. The OCT B-scan through the fovea of each patient was graded based on the morphology of the inner–outer segment (IS/OS) junction layer according to a previously proposed classification: (1) IS/OS junction disorganization in the fovea, (2) IS/OS junction loss in the fovea, and (3) extensive loss of IS/OS junction (more than 1 disc diameter from the fovea).[9,10] The average retinal thickness within a 1-mm diameter ring centered in the fovea was determined using the Heidelberg Spectralis software on the last imaging occasion, for each patient with volume OCT scan.

Electrophysiology

Full field electroretinography (ERG) was performed to incorporate the standards of the International Society for Clinical Electrophysiology of Vision (ISCEV)[11] in 12, 15, and 19 patients from groups A to C, respectively. The data were ususally symmetrical and those from the right eye were used for analysis. Patients were classified according the full-field ERG findings into one of three groups:[12] normal (group 1; dysfunction confined to the macula), generalized cone system dysfunction (group 2), or cone and rod system dysfunction (group 3). The DA 0.01, DA 10.0, LA 3.0 30 Hz, and LA 3.0 single flash amplitudes and LA 3.0 30 Hz peak times were analyzed using linear regression to estimate the rates of age-related decline. The 95% confidence interval of group A for DA a-wave and LA 3.0 30 Hz amplitudes, representing mostly rod and cone system function, respectively, were used to determine whether the splicing mutations resulted in a null-like or comparatively milder phenotype. The ERG values of age-matched controls ($N = 150$) incorporating previously published normative data[13,14] were used for reference. Two children were tested using periorbital surface electrodes according to a previously published pediatric protocol.[15] They were included into analysis of ERG groups but were omitted from quantitative analysis.

Genetic Analysis

The majority of genotypes were ascertained by next generation sequencing as a part of a retinal panel at Casey Eye Institute. Specifically, direct testing for mutations in the genes of the Stargardt/Macular dystrophy SmartPanel v4 (613 primer sets) was performed by PCR amplification and Next Generation Sequencing. Polymerase chain reaction primer sets were printed onto a specific chip. Each primer set was duplicated on the chips to avoid random PCR failure. Any low coverage region (<×100) was covered afterwards by PCR and Sanger sequencing. Identified mutations and novel variations were confirmed by Sanger sequencing. Phase of the two variants was explored when relatives were available, and in each case confirmed they were in trans. Effect on splicing was tested using the Human Splicing Finder program, version 3.0 (available in the public domain at umd.be/HSF3/). The nine studied splicing mutations of group B patients are presented in Table 1. Mutations in each patient are shown in the Supplementary Table S1.

Statistical Analysis

Statistical analysis was performed using SPSS software v. 22 (IBM SPSS Statistics; IBM Corporation, Chicago, IL, USA). The Mann-Whitney *U* test with Bonferroni correction was used to compare the median age at onset of groups B and C patients to that of group A patients, and the median age at onset of

Investigative Ophthalmology & Visual Science

Table 1. Predicted Effects on Splicing and Results of Functional Studies of Studied Splice-Site Mutations

Nucleotide Change	*N* of Alleles	Intron	Human Splicing Finder (HSF3) Analysis*	Previously Reported	Functional Studies
c.768 G>T (*P*.V256V)	1	End of exon 6	Alteration of the WT donor site, most probably affecting splicing	Maugeri et al.[17]	Total lack of normally spliced mRNA transcript[17]
c.859-9T>C	2	7	No significant splicing motif alteration detected	Allikmets et al.[18]	
c.4253+4C>T	2	28	Activation of an intronic cryptic donor site	Webster et al.[19]	
c.5196+1G>A	2	36	Alteration of the WT donor site, most probably affecting splicing	Shroyer et al.[27]	
c.5461-10T>C	11	38	No significant splicing motif alteration detected	Klevering et al.[20]	Skipping of exon 39 or exons 39 and 40 resulting in premature stop codons[21]
c.5714+5G>A	4	40	Alteration of the WT donor site, most probably affecting splicing.	Cremers 1998[36]	Partial lack of normally spliced mRNA transcript[22]
c.6479+1G>A	4	47	Alteration of the WT donor site, most probably affecting splicing.	Zernant et al.[23]	
c.6729+4_c.6729+18del15†	12	48	Alteration of the WT donor site, most probably affecting splicing.	Littink et al.[24]	
c.6817-2A>C	1	49	Alteration of the WT acceptor site, most probably affecting splicing.	Fujinami et al.[4]	

All splicing mutations were located within the classical consensus splicing region.[16]
* Available in the Public Domain at http://www.umd.be/HSF3/.
† Changes the splicing consensus region +5 (g>c) and +6 (g>c).

patients with splicing mutation c.5714+5G>A and patients with other splicing mutations to that of group A patients. Pearson correlation was used to test relationships between age and the area of reduced autofluorescence, and between age and ERG amplitudes. Analysis of covariance (ANCOVA) with post hoc test was used evaluate the differences between the slopes of regression lines. The Wilcoxon test with pairwise comparisons was used to test for significant differences among VA Kaplan Meier curves of different patient groups. Multiple regression analysis was used to assess the relationship between the average macular thickness, different genotypes, and age. The Kruskal-Wallis test with post hoc pairwise comparisons was used to compare the frequency of extensive Increased Size Exclusion Limit (ISe) loss between different genotypic groups. The research adhered to the tenets of the Declaration of Helsinki.

Results

Age of Onset

The median age at onset of visual symptoms was 6, 8, and 17 years for groups A to C, respectively. When patients harboring different splicing mutations were individually compared to the nullizygous group (group A), the ones with mutation c.5714+5G>A had significantly later median age of onset (Mann-Whitney *U* test, $P < 0.05$; Fig. 2).

Visual Acuity

Visual acuity was the same in both eyes in 56% (36/64) of patients, and within ≤0.3 logMAR difference between the right and left eyes in 92% (59/64). The level of VA plotted against age for different genotypes is shown in Figure 3. At the last follow-up, the median VA of the better eye was 1.3 logMAR (range, 0.78 to light perception) in group A, 1.11 logMAR (range, 0.48 to counting fingers; median age, 19 years) in group B, and 0.9 logMAR (range, 0.18–1.78) in group C. Thus, at the last follow-up visit at the median ages of 19 years in groups A and B, 74% (14/19) in group A and 58% (15/26) in group B patients had VA > 1 logMAR (20/200), compared to 16% (3/19) in group C at the median age of 36 years. Within groups A and B, no patient older than 40 years had VA better than 20/600 (1.48 logMAR), with the exception of one 48-year-old group B patient with c.5714+5G>A (VA 20/200). Kaplan Meier survival analysis estimated that 50% of patients reached VA worse than 20/400 (1.3 logMAR) at the age of 29 years for group A (95% CI 23–35 years), 48 years for group B (95% CI 34–62 years), and 66 years for group C (95% CI 58–74 years; Fig. 3C). The difference between groups was significant (Wilcoxon test, $P < 0.05$). When the three most common mutations were analyzed separately, the survival curve for mutation c.5714+5G>A was significantly different from group A ($P < 0.05$), whereas the curves for c.5461-10T>C and c.6729+4del15 did not differ significantly.

Clinical Presentation

Funduscopy revealed different stages of retinal dystrophy (Fig. 4). Characteristic yellow flecks were observed in 3/19 patients from group A (ages 8–10 years) and 6/27 from group B (ages 9–22 years). They extended beyond the vascular arcades in all cases (Fishman stage II). Two of those patients first presented with a normal fundus at the ages of 7 and 9 years, with flecks appearing 1 to 2 years later. Two other patients from groups A and B first presented with a central atrophic lesion but no flecks at the age of 10 and 7 years, respectively. Other patients without flecks had signs of RPE and/or chorioretinal atrophy outside the macular lesion, with pigmentary deposition (Fishman stages III, IV). Among 20 patients from group C, 17 were classified into stages 0 or 1, three had flecks extending outside the vascular arcades (Fishman II), and none had significant RPE atrophy outside the central lesion (Fishman III, IV).

Investigative Ophthalmology & Visual Science

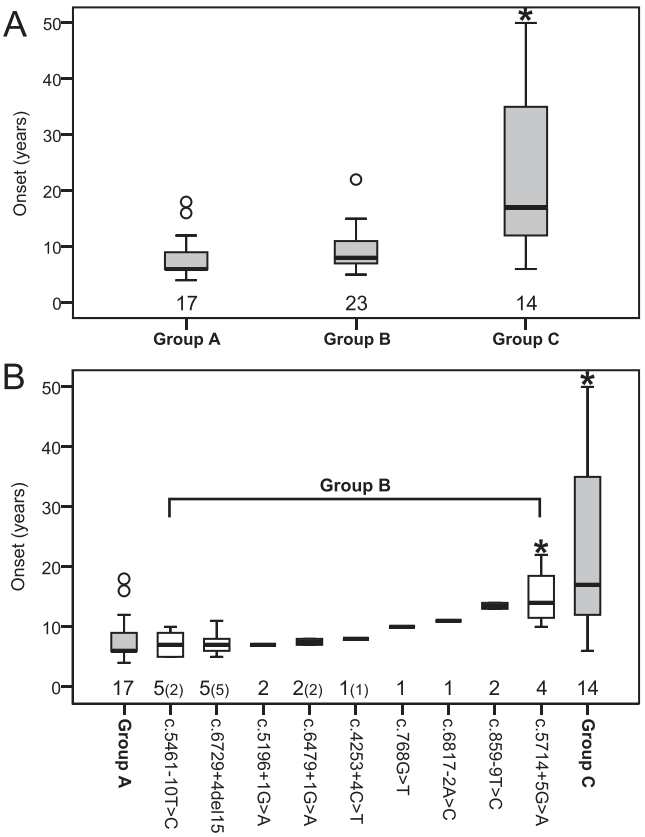

Figure 2. Boxplot charts of disease onset. (**A**) Disease onset for different studied patient groups. (**B**) The same chart with splicing mutations from group B shown separately, ordered from the earliest to the latest onset. *Horizontal lines* represent the median values, boxes represent half of the data for each group/mutation, and *whiskers* represent the remaining data except in the case of the outliers (*circles*). The number of patients for each genotype is indicated below each box, with those homozygous for splicing mutations appearing in parentheses. Group C patients and the patients with splicing mutation c.5714+5G>A had significantly later disease onset than Group A patients (shown by *asterisks*; Mann-Whitney *U* test, $P < 0.05$). Mutation c.859-9T>C also was associated with notably later onset, but the number of patients was too few for statistical analysis.

FAF and OCT

There were various patterns of abnormally increased and/or decreased FAF in all patients. Similar patterns were present in patients of similar age within groups A and B, and progression from one pattern to another could occur (Fig. 5). The correlation between the total area of decreased autofluorescence within the 30° × 30° FAF image and age was significant for groups A and B (Pearson's correlation, $R = 0.83$ and 0.86, respectively; $P < 0.001$ for both) but not for group C (Pearson's correlation, $R = 0.17$, $P = 0.48$). Figure 6 shows the area of reduced FAF plotted against age. Assuming linear expansion of the low density FAF area, the regression line for group A estimated total involvement of the 30° × 30° area at the age of 53 years. Using the 95% nullizygous confidence interval, three patients were noted to have significantly smaller areas of reduced FAF; they carried c.5714+5G>A in trans with a null ($N = 2$) and p.V256V in trans with a null ($N = 1$). Table 2 shows the yearly enlargement rates estimated from the cross-sectional data ($N = 58$) and the median measured enlargement in those for whom longitudinal data were available ($N = 36$).

The average macular thickness in the central 1 mm was 133 ± 21, 121 ± 21, and 137 ± 39 μm, for groups A to C at the median ages of 19, 16, and 35 years, respectively. The difference among groups was not significant (multiple linear regression analysis with correction for age, $P = 0.15$). Loss of ISe extending more than one disc diameter from the fovea was observed in 100% (14/14) of patients from group A, 95% (22/23) from group B, and 24% (4/17) from group C. The lower frequency in group C was statistically significant (Kruskal-Wallis with pairwise comparisons, $P < 0.001$).

Full-Field ERG

The incidence of different ERG groups appears in Table 3. Electroretinography groups 1 to 3 were observed in 1/12, 1/12, and 10/12 patients in group A, and 1/15, 1/15, and 13/15 in group B, respectively. All patients from group C had normal full-field ERG (ERG group1). Within group A, the patient with a normal full-field ERG was 10 years old, 4 years after onset, and had normal FAF outside a relatively large central lesion (Fig. 7). The patient with ERG group 2 was 7 years old, 1 year after onset, and had normal FAF outside the central lesion (Fig. 7). Three other group A patients were examined within 4 years of disease onset, all had ERG group 3 and abnormal FAF outside the central lesion. Within group B, the patient with normal full-field ERG was 24 years old, 2 years after onset, had abnormal FAF outside the central lesion, and carried c.5714+5G>A in trans with a null allele. The patient with ERG group 2 was 8 years old, 2 years after onset, and had normal FAF outside the central lesion (Fig. 7). Seven other group B patients were examined within 4 years after onset, all had ERG group 3, and had abnormal FAF outside the central lesion. Table 4 shows correlations between the major ERG parameters and age for

Table 2. Median Rate of Enlargement of the Area of Decreased Autofluorescence Derived From the Longitudinal and Cross-Sectional Data

Group/ Mutation	Enlargement Rate in Patients With Follow-Up, Median (Range, mm²/y)	*N*	Statistically Different From Group A (Mann-Whitney *U* Test)	Enlargement Rate Determined by the Slope of the Cross-Sectional Regression Lines, mm²/y	*N*	Statistically Different From Group A (ANCOVA)
A	1.4 (0.2–3.7)	5		1.5	14	
B	0.9 (0.2–3.7)	14	No ($P = 0.30$)	1.2	24	Yes ($P < 0.05$)
	0.7* (0.2–2.7)	12	No ($P = 0.20$)	1.3*	21	Yes ($P < 0.05$)
-c.5461-10T>C	1.3 (−0.61 to −3.24)	3(1)	No ($P = 0.27$)	1.3	7(3)	No ($P = 0.09$)
.6729+4del15	N/A			1.4	5(5)	No ($P = 0.59$)
C	0.06 (0.00–0.77)	17	Yes ($P < 0.05$)	0.03	20	Yes ($P < 0.05$)

Splicing mutations with data from at least 3 patients are shown separately with the number of homozygous patients shown in brackets. For the longitudinal data, the rate of enlargement was calculated as the enlargement of the area of decreased autofluorescence divided by the number of follow-up years. For the cross-sectional data the rate was determined from the regression line equation.

* Excluding c.5714+5G>A.

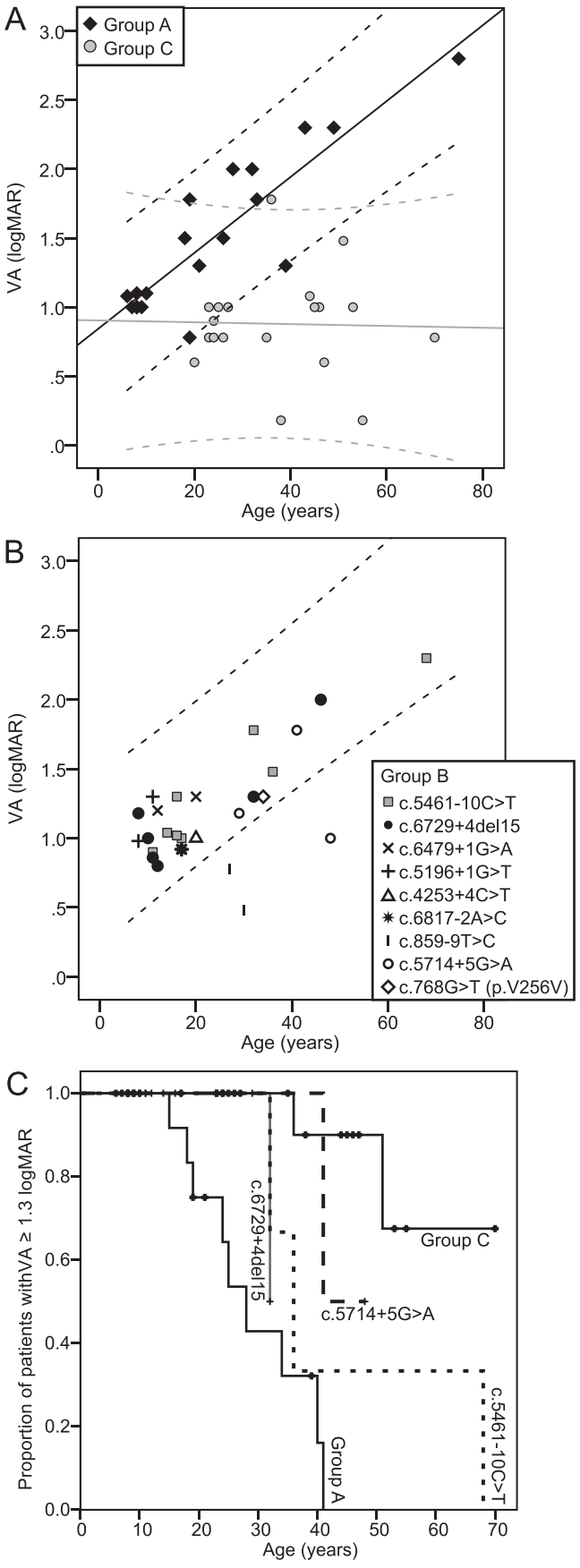

Figure 3. (**A**) Visual acuity of the better eye of patients from groups A and C at their last visit. *Solid black line* represents the regression line of group A and *dashed lines* its 95% CI. The majority of patients from group A had VA worse than 1.3 logMAR (20/400) (**B**) Visual acuity of patients from group B with individual splicing mutations marked with different symbols. The regression line and 95% CI of group A is plotted for reference. The three patients with significantly better VA in comparison to group A patients carried mutations c.859-9T>C ($N = 2$) and c.5714+5G>A ($N = 1$). (**C**) Survival analysis showing the probability of retaining VA of $\geq$ 20/400 (1.3 logMAR) for group A, group C, and the three most common splicing mutations. The survival curve for mutation c.5714+5G>A differs significantly from group A ($P < 0.05$).

the studied groups and the linear regression slopes (equations), used to estimate the yearly rates of ERG amplitude decrease. Among the parameters reflecting mostly rod and cone function, respectively, the DA 10.0 ERG a-wave and LA 3.0 30 Hz amplitudes were correlated most consistently with age in groups A and B (excluding c.5714+5G>A), while no parameter correlated with age in group C (see Fig. 8). Using the 95% nullizygous confidence interval, three patients had significantly higher DA 10.0 and LA 3.0 30 Hz amplitudes; all carried mutation c.5714+5G>A in trans with a null. Two patients had higher DA 10.0 but not LA 3.0 30 Hz amplitudes; one carried c.859-9T>C in trans with a null, and the other was homozygous for c.6729+4del15. Analysis of covariance showed the regression slopes of DA 10.0 ERG a-wave and LA 3.0 30 Hz were significantly different among groups A, B (excluding c.5714+5G>A), C, and healthy controls ($P < 0.05$ for all pairwise comparisons). The other ERG parameters (DA 0.01, DA 10.0 b-wave, LA 3.0 a-, and b-wave amplitudes; and LA 3.0 30 Hz peak times) are reviewed in Supplementary Figure S1.

Discussion

This study characterizes the phenotype and rates of progression associated with nullizygosity for *ABCA4* and with that an absence of ABCA4 protein. Using the latter as a comparator group, the study further demonstrated that most splicing mutations result in a null-like phenotype (within 95% CIs for onset, VA, FAF, and ERG), with a notable exception of c.5714+5G>A, which is associated with a significantly milder phenotype.

The nullizygous phenotype was that of an early onset, rapidly progressing cone–rod dystrophy. The VA in ABCA4-retinopathy usually stabilizes at the level of 20/200 to 20/400,[25] with Fishman phenotypes II and III,[26] and early disease onset[3,7] often associated with a more severe visual decline. The present data showed that the nullizygous patients are at a very high risk of VA loss beyond 20/400 (1.3 log MAR) by the fourth decade, establishing an additional genetic predictor for severe visual loss. Decreased FAF is a commonly used marker of retinal degeneration in ABCA4 retinopathy. The estimated rates of enlargement of reduced FAF areas in nullizygous patients (1.4–1.5 mm^2/y) were comparable with the higher end of the range reported by Chen et al. (0.2–2.1 mm^2/y),[27] the rates reported for similar FAF patterns (0.7–4.4 mm^2/y),[28] and the rates reported for ERG group 3 (2.3 mm^2/y),[29] highlighting the utility of this parameter for assessing progressive maculopathy in ABCA4-retinopathy. The estimated rates of progression for p.G1961E patients were significantly slower (0.03–0.06 mm^2/y), highlighting the importance of considering the genotype in future clinical studies, especially involving patients with otherwise overlapping characteristics (e.g., early disease onset). For example, Testa et al.[10] reported an average RPE lesion area enlargement in patients with juvenile Stargardt disease (mean disease onset of 15 years) to be 0.3 mm^2/y; however, more than a third of their patients (22/56) carried mutation p.G1961E, likely lowering the average rate

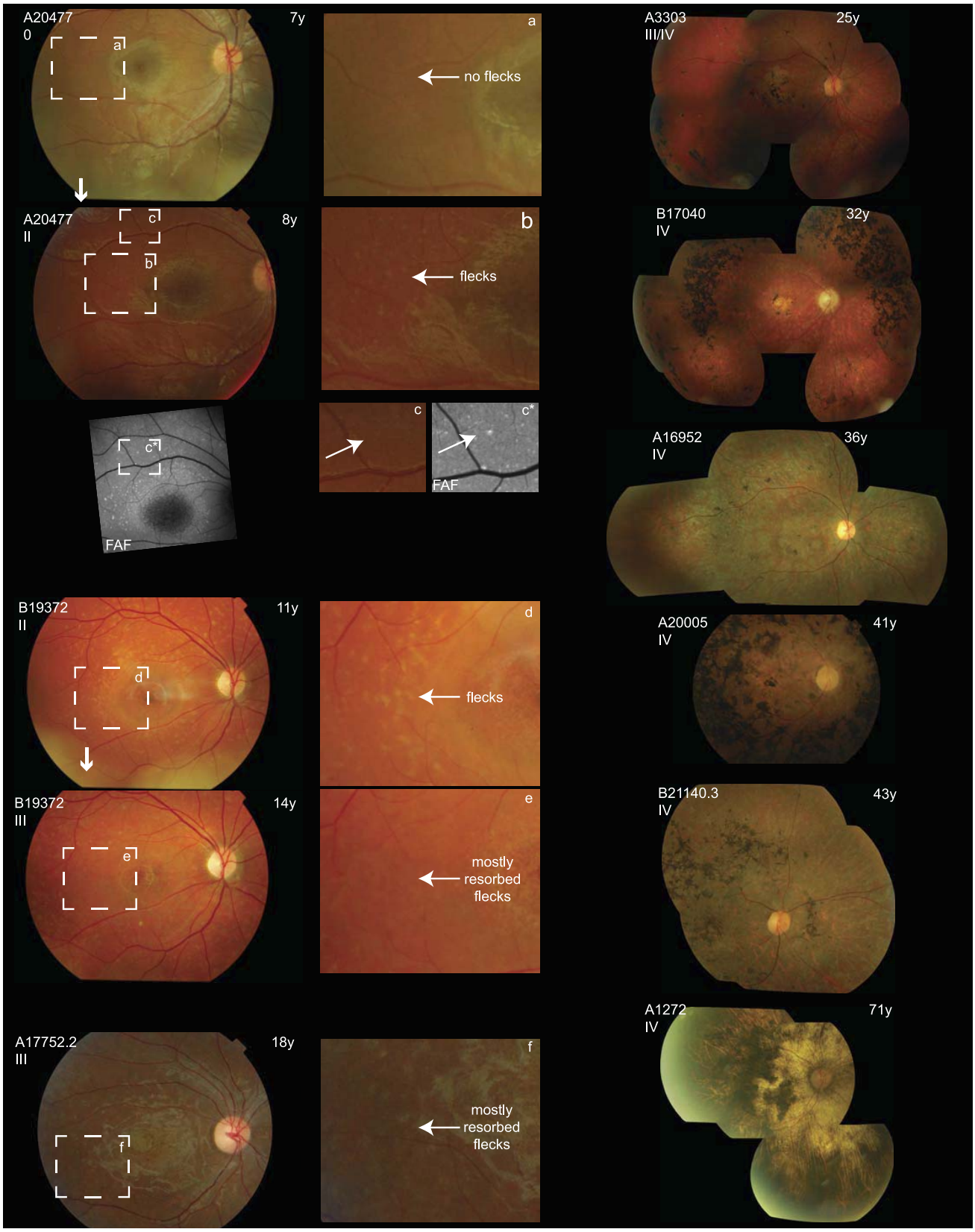

Figure 4. Representative fundus images of patients from groups A and B. The patient number is noted in the *top left corner* and age in the *top right corner* of each fundus image. Fishman group classification is shown in *roman numerals*. The first two columns show patients younger than 20 years. Two patients showed progression from one stage to another on follow-up (*arrows*); patient 31599 from normal fundus to group II (flecks outside the arcades can be seen better on the FAF image, c*) and 30062 (stages II–III). *Dashed rectangles* mark the areas shown enlarged in the *second column*. The *third column* shows images of patients older than 20 years, with some of the most advanced cases resembling a retinitis pigmentosa phenotype. No patient had flecks limited to the vascular arcades (Fishman I).

Investigative Ophthalmology & Visual Science

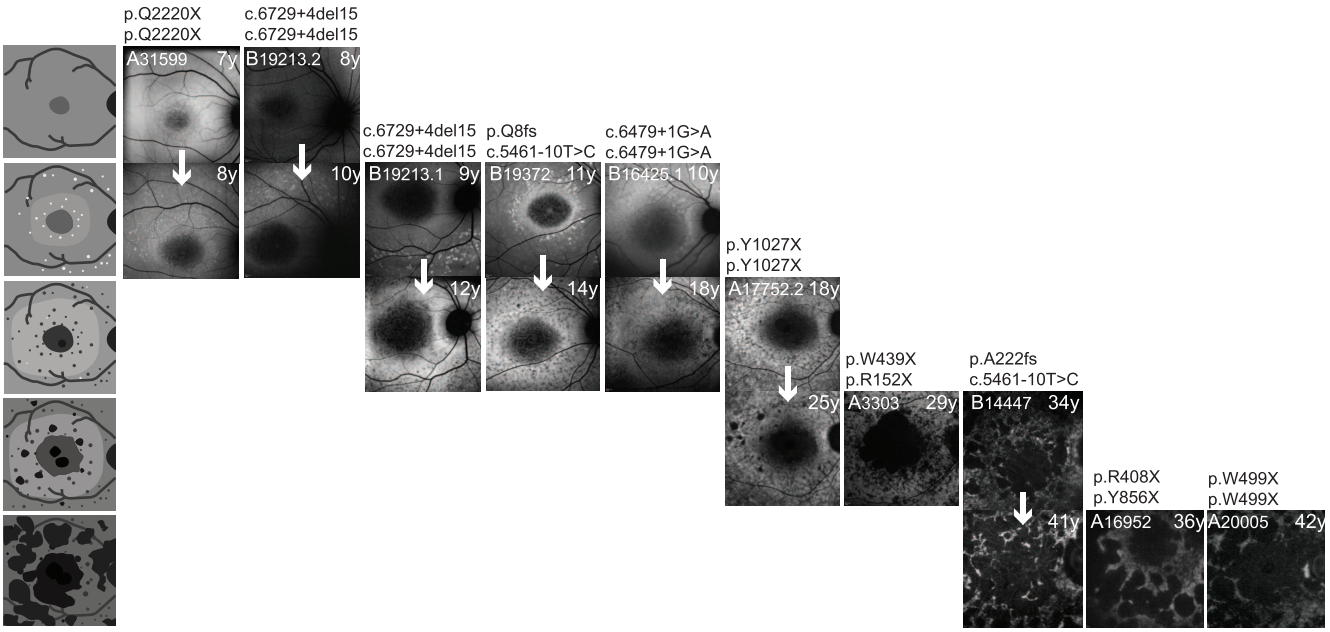

Figure 5. First column shows the model of FAF progression associated with two null or likely-null alleles, based on qualitative analysis of the FAF shown in the other columns; FAF images are shown in patients from groups A and B (excluding c.5714+5G>A). Similar FAF patterns are aligned horizontally, revealing an age-related trend. Longitudinal imaging in 6 patients showed progression from one FAF pattern to another (positioned *vertically*, marked with *arrows*). The earliest sign is a centrally decreased or irregular autofluorescence, followed by the appearance of multiple foci of increased signal, observed at approximately 10 years of age. Foci of increased FAF are replaced by *dark spots* of decreased FAF which enlarge and coalesce over time. By the fifth decade, there is severe widespread and patchy loss of FAF. Note the absence of characteristic peripapillary sparing in some of the older patients. The patient number is noted in the *top left corner*; age in the *top right corner* of the FAF image. Genotypes are stated above each image.

of progression. Full-field ERG provides an objective measure of peripheral retinal involvement. Three functional phenotypic subtypes were established previously[12] (see Methods) and a longitudinal follow-up of the same cohort (mean follow-up 11 years) found that only 20% of ERG group 1 (normal full-field ERG) cases had progression to either group 2 or 3 (cone and cone–rod dystrophy, respectively), whereas 100% of patients with initial rod ERG abnormality showed significant progression. The correlation between genotype and ERG is poorly understood and difficult to explore due to the genetic heterogeneity of *ABCA4*. Two studies of 76 and 198 Stargardt patients, respectively, reported a higher frequency of two identified ABCA4 variants in patients with severe ERG phenotypes.[30,31] In another study a limited genotype–phenotype analysis suggested a higher prevalence of ERG group 3 and higher risk of deterioration for patients harboring null variants.[32] The current study expanded those findings and showed that the majority of patients harboring two null variants, presented with ERG group 3, except two with $\leq$4 years of disease duration (both with normal FAF outside the central lesion). The further cross-sectional analysis of ERG amplitudes revealed a rapid age-related decline reaching nondetectable levels by the fifth decade in this genetic subgroup, corresponding with the widespread retinal degeneration observed clinically (Fishman stage IV, severely abnormal FAF). Oh et al.[31] observed a higher incidence of abnormal ERGs in patients with clinically widespread lesions; however, normal ERG could also be observed in some.[31] In this study, there was a consistent association between widespread flecks or FAF abnormalities and abnormal ERGs within the nullizygous group. On the contrary, all the p.G1961E patients had normal ERGs, even in cases when flecks extended beyond the vascular arcades. One of the c.5714+5G>A patients also displayed widespread

Table 3. Distribution of Different ERG Groups Among Patients From Groups A to C, and Their Clinical Characteristics

	Group A, Biallelic Null Mutation		Group B, Splicing Mutations in a Homozygous State or in Trans With a Null Mutation		Group C, p.G1961E in Trans With a Likely-Null Mutation	
ERG Group	***N***	**Clinical Group**	***N***	**Clinical Group**	***N***	**Clinical Group**
Group 1, normal full field ERG	1	Fishman 0	1*	Fishman II	19	Fishman 0–II
Group 2, abnormal cone ERGs	1	Fishman 0	1	Fishman 0	0	N/A
Group 3, abnormal cone and rod ERGs	10	Fishman II-IV	13	Fishman 0–IV	0	N/A

All patients, including the ones with Fishman 0 on fundus exam had an abnormal FAF and/or notable loss of photoreceptors on OCT (shown in Fig. 7 for groups A and B patients). N/A, not applicable.

* c.5714+5G>A in trans with a null mutation.

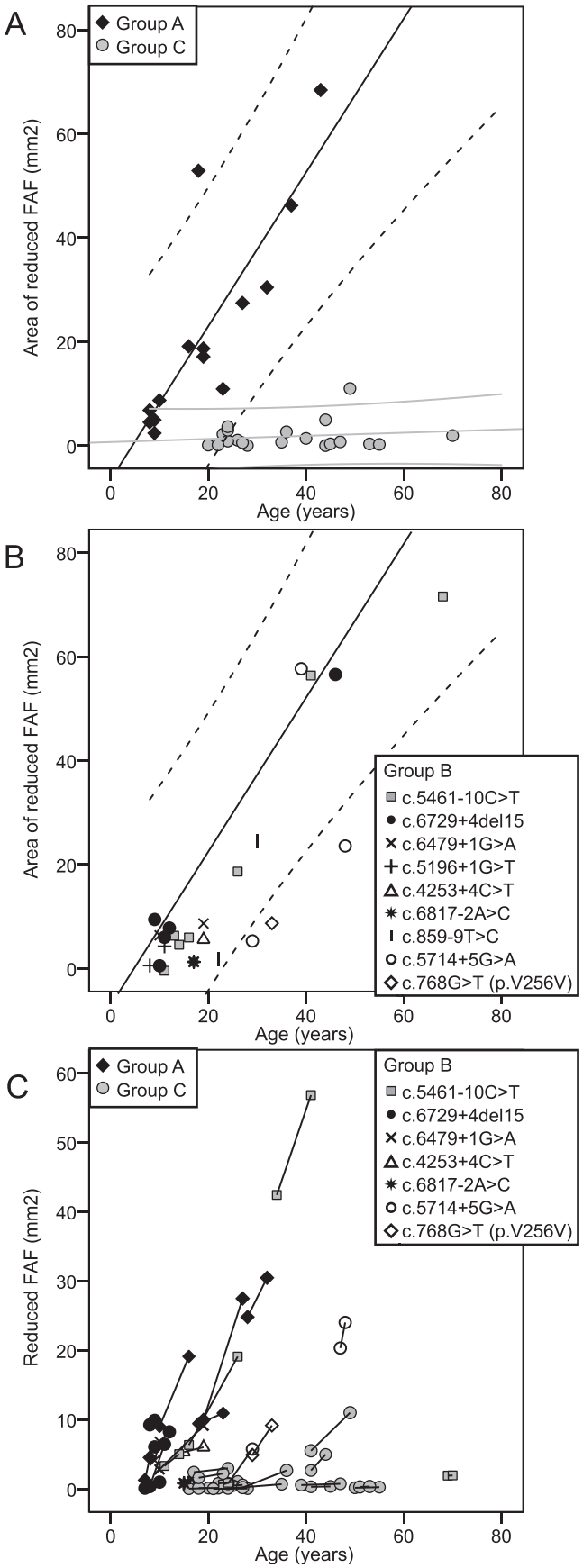

Figure 6. (**A**) Cross-sectional scatter plot showing the total area of reduced FAF of the right eye at their last visit plotted against age for patients from groups A and C. *Full black line* represents the regression line for group A and *dashed lines* its 95% CI. (**B**) Area of reduced FAF of patients from group B with individual splicing mutations marked with different *symbols*. The regression line and 95% CI of group A is plotted for reference. Three group B patients differed significantly from group A including two patients harboring mutation c.5714+5G>A. (**C**) Spaghetti plot showing the increase of the area of reduced FAF in patients followed longitudinally. Note that even though most of group B had small areas of reduced FAF, they were comparatively younger than patients from group C, reflecting the earlier disease onset.

FAF and had normal ERG. Further careful studies of the type and extent of flecks/FAF abnormalities in different genotypes are needed to understand those associations, which may reflect different disease mechanisms. The main cause of loss of photoreceptors is thought to be RPE dysfunction due to accumulation of bisretinoids, corresponding to yellow/hyperautofluorescent flecks. Direct cone toxicity related to the cone open membrane structure was proposed as an additional contributing mechanism.[33] The nullizygous patients provide an insight into the path of retinal degeneration occurring in the total absence of ABCA4. The primary visual symptom of those patients was reduced VA, occurring at a median age of 6 years, and the leading structural defect observed on OCT was photoreceptor loss in the cone-rich region of fovea and parafovea without obvious RPE involvement (Fig. 7), suggesting cones in those areas as the primary disease target. The peripheral photoreceptors become involved soon afterwards, as shown by abnormal full-field ERG in all patients older than 10 years (all patients with more than 5 years of disease duration). It is curious that one patient with ERG group 2 and one with ERG 3 had seemingly normal FAF outside the central lesion, suggesting that at least in those cases there was no major RPE lipofuscin accumulation at that time and supporting the idea of the direct cone toxicity. It also is noteworthy that flecks were observed only in patients aged approximately 10 years, were not well defined, and were rapidly replaced with RPE and photoreceptor atrophy. A substantial contribution of primary photoreceptor loss in nullizygous patients is consistent with the postmortem evaluation of a human donor eye harboring two likely null mutations (p.F1440fs and c.2160+1G>C), which at 78 years of age revealed loss of the outer nuclear layer over the whole retina with regional preservation of the RPE.[34] That the cones were relatively more endangered compared to rods was suggested by studies on a *ABCA4*$^{-/-}$/*Nrl*$^{-/-}$ mouse model, which indicated that ABCA4-deficient cones simultaneously generate more A2E than rods and are less able to effectively clear it.[33] The advantage of a genotype–phenotype correlation study using strict genetic inclusion criteria is the capacity to discover the range of phenotypes associated with a specific genotype. The phenotype of nullizygous patients proved to be consistently severe; however, there was a certain range for all of the studied parameters and a few outliers (e.g., two patients with onset age $>$ 15 years and a patient with significantly better visual acuity. The comparator group harboring mutation p.G1961E, while demonstrating a mild phenotype, also exhibited some variability, especially for disease onset and ERG amplitudes. The reason for the variability, extrinsic to the ABCA4 genotype, is not yet established, but may be related to variants in other genes or environmental factors.

Splicing Mutations

Splicing mutations in general can have various consequences on RNA processing, such as exon skipping, intron inclusion, and leaky splicing.[35] In the latter, a considerable amount of

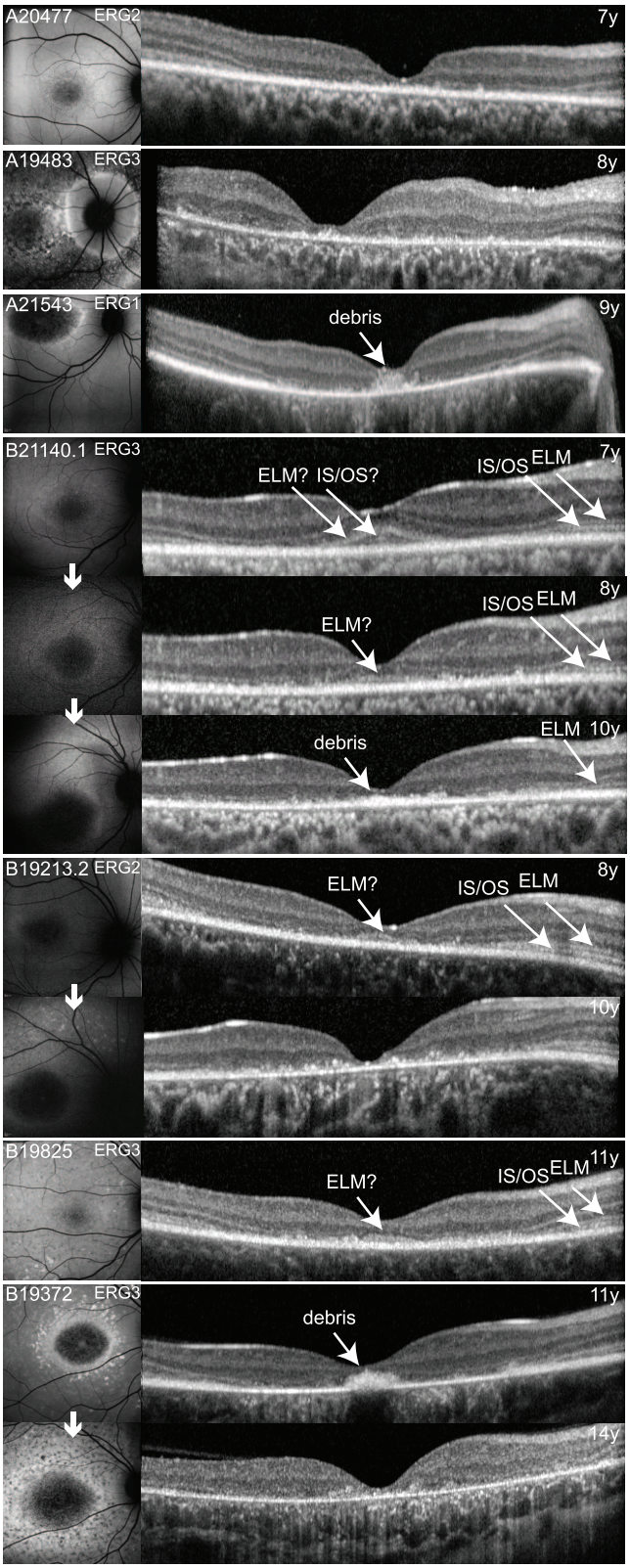

Figure 7. Fundus autofluorescence and OCT images of the youngest patients from groups A (*top three patients*) and B (*bottom three patients*), ages 7 to 11 years. Follow-up images are marked with *arrows*. Optical coherence tomography showed loss of outer retinal structure in the central macula of all patients, even those with only subtle FAF changes. A residual OCT band resembling the external limiting membrane (ELM) was observed in the fovea of three patients, suggesting primary parafoveal damage. Hyperreflective material marked as debris was present in the fovea of two patients, which disappeared after 2 years of follow-up in one patient. The ERG group is noted in the *top right corner* of the FAF image. Note the seemingly normal FAF outside the central lesions in patients with ERG groups 1 and 2, as well one patient with ERG 3.

normally spliced product can still be produced, and this has been demonstrated previously in vitro for one of the studied splicing mutations, c.5714+5G>A.[22] Four patients harboring this variant in trans with a null mutation were included in the study, and comparison with nullizygous patients revealed significant difference for all parameters, confirming previous reports of relatively mild phenotype associated with the variant.[2,36,37] Conversely, other studied mutations (c.5461-10T>C, c.6729+4del15, c.4253+4C>T, c.5196+1G>A, and c.6479+1G>A, c.6817-2A>C, c.859-9T>C, and c.768G>T) resulted in a null-like phenotype in the the majority of cases. Inspection of onset distributions and cross-sectional plots for VA, FAF, and ERG revealed a modest trend toward a milder phenotype in some cases; however, rarely extending over past the nullizygous 95% CI (exceptions included c.6817-2A>C for onset, c.768G>T for FAF and c.859-9T>C for onset and VA). Interestingly, Cideciyan et al.[37] suggested an earlier onset of retina-wide disease for c.5461-10T>C compared to the nullizygous patients, as deduced from longitudinal analysis of visual fields. This is of importance, because c.5461-10T>C is one of the most prevalent *ABCA4* variants.[19] A considerably large number of patients harboring this variant in a homozygous state ($N = 3$) or in trans with a null mutation ($N = 5$) are included in the present study, and a well-defined nullizygous comparator group provided substantial evidence that the associated phenotype is well within the nullizygous phenotype.

Conclusions

Nullizygosity for *ABCA4* is characterized by early involvement of foveal cones as well as early involvement of peripheral retina. There was a rapid progression of disease shown by enlargement of central atrophy on FAF imaging and decline of ERG amplitudes with age, and patients were at high risk of reaching legal blindness by the fourth decade. Most splicing mutations showed minimal or no difference to the null phenotype, but the mutation c.5714+5G>A was associated with a significantly milder phenotype. The strict genetic inclusion criteria resulted in a set of phenotypic data describing disease onset, VA, FAF, and ERG characteristics, which can be helpful in a clinical setting and may inform the design and interpretation of novel treatment trials.

Acknowledgments

Supported by the National Institute for Health Research Rare Diseases Translational Research Collaboration (NIHR RD-TRC; Cambridge, UK) and NIHR Moorfields Biomedical Research Centre (London, UK), UCL Institute of Ophthalmology (London, UK), and by Fight for Sight (London, UK) and Foundation Fighting Blindness (Columbia, MD, USA). The authors alone are responsible for the content and writing of this paper.

Disclosure: **A. Fakin**, None; **A.G. Robson**, None; **K. Fujinami**, None; **A.T. Moore**, None; **M. Michaelides**, None; **J.(P.-W.) Chiang**, None; **G.E. Holder**, None; **A.R. Webster**, None

Table 4. Correlation Between ERG Parameters and Age for Different Groups of Patients

	Correlation With Age, Pearson Coefficient					Estimated Yearly Decline, Linear Regression			
	A	B	B excl. c.5714+5G>A	C	Healthy Controls	A	B excl. c.5714+5G>A	C	Healthy Controls
DA 0.01 b-wave ampl.	−0.68*	0.16	−0.31	−0.13	−0.64*	−4.9 μV	−3.6 μV	−0.8 μV	−2.1 μV
DA 10.0 a-wave ampl.	−0.67*	−0.21	−0.60*	−0.41	−0.53*	−3.5 μV	−6.1 μV	−1.8 μV	−1.5 μV
DA 10.0 b-wave ampl.	−0.74*	−0.28	−0.75*	−0.06	−0.46*	−5.1 μV	−9.6 μV	+0.5 μV	−2.1 μV
LA 30 Hz ampl.	−0.63*	0.12	−0.65*	−0.34	−0.47*	−0.9 μV	−1.4 μV	−0.8 μV	−0.7 μV
LA 30 Hz peak time	0.40	−0.22	0.29	−0.18	0.44*	+0.2 ms	+0.2 ms	+0.0 ms	+0.05 ms
LA 3.0 a-wave ampl.	−0.49	−0.23	−0.63*	−0.10	−0.44*	−0.2 μV	−0.9 μV	−0.1 μV	−0.2 μV
LA 3.0 b-wave ampl.	−0.58	−0.07	−0.57	−0.36	−0.53*	−0.8 μV	−2.1 μV	−1.5 μV	−1.0 μV

* Significant correlations (Pearson coefficient). The yearly decline for each parameter was estimated using linear regression.

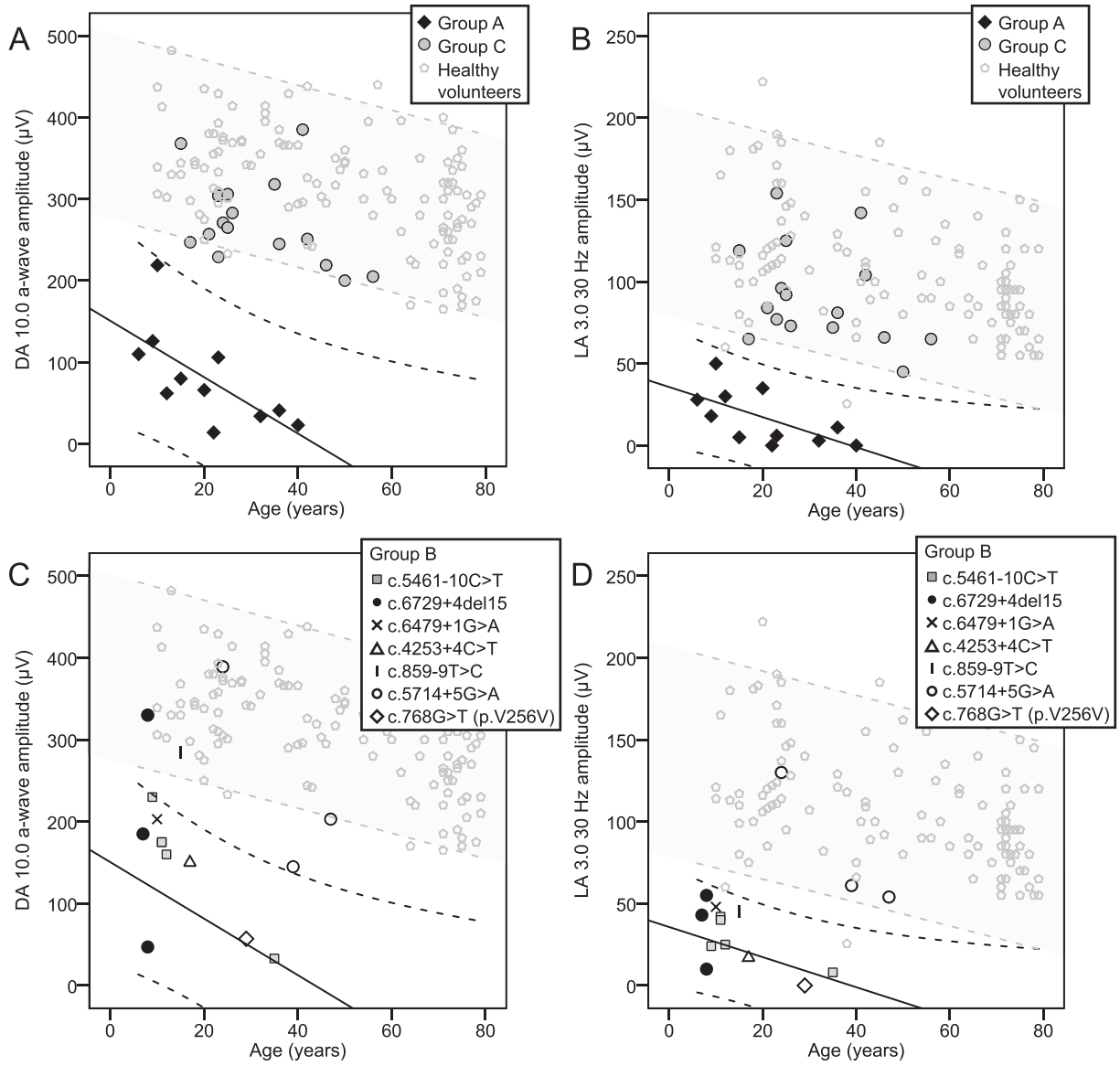

Figure 8. (**A**, **B**) Cross-sectional scatter plot showing the ERG amplitudes for dark adapted 10.0 ERG a-wave (predominantly reflecting rod function [**A**]) and light adapted 3.0 30 Hz response (reflecting cone system function [**B**]) in relation to age for groups A and C**.** *Full line* represents the regression line of group A and *dashed lines* its 95% CI. (**C**, **D**) The same ERG parameters as above, plotted for patients from group B with individual splicing mutations marked with different *symbols*. The regression line and 95% CI of group A is plotted for reference. The *gray area* represents the 95% CI of healthy controls. Electroretinography of two patients from group A are not shown because they were examined using surface electrodes. They were ERG groups 1 and 2, respectively.

Investigative Ophthalmology & Visual Science

References

1. Dalkara D, Goureau O, Marazova K, Sahel JA. Let there be light: gene and cell therapy for blindness. *Hum Gene Ther*. 2016;27:134–147.
2. van Driel MA, Maugeri A, Klevering BJ, Hoyng CB, Cremers FP. ABCR unites what ophthalmologists divide(s). *Ophthal Genet*. 1998;19:117–122.
3. Lambertus S, van Huet RA, Bax NM, et al. Early-onset stargardt disease: phenotypic and genotypic characteristics. *Ophthalmology*. 2015;122:335–344.
4. Fujinami K, Zernant J, Chana RK, et al. Clinical and molecular characteristics of childhood-onset Stargardt disease. *Ophthalmology*. 2015;122:326–334.
5. Lange C, Feltgen N, Junker B, Schulze-Bonsel K, Bach M. Resolving the clinical acuity categories "hand motion" and "counting fingers" using the Freiburg Visual Acuity Test (FrACT). *Graef Arch Clin Exp Ophthalmol*. 2009;247:137–142.
6. Grover S, Fishman GA, Anderson RJ, et al. Visual acuity impairment in patients with retinitis pigmentosa at age 45 years or older. *Ophthalmology*. 1999;106:1780–1785.
7. Rotenstreich Y, Fishman GA, Anderson RJ. Visual acuity loss and clinical observations in a large series of patients with Stargardt disease. *Ophthalmology*. 2003;110:1151–1158.
8. Kuehlewein L, Hariri AH, Ho A, et al. Comparison of manual and semiautomated fundus autofluorescence analysis of macular atrophy in Stargardt disease phenotype. *Retina*. 2016;36:1216–1231.
9. Testa F, Rossi S, Sodi A, et al. Correlation between photoreceptor layer integrity and visual function in patients with Stargardt disease: implications for gene therapy. *Invest Ophthalmol Vis Sci*. 2012;53:4409–4415.
10. Testa F, Melillo P, Di Iorio V, et al. Macular function and morphologic features in juvenile stargardt disease: longitudinal study. *Ophthalmology*. 2014;121:2399–2405.
11. McCulloch DL, Marmor MF, Brigell MG, et al. ISCEV Standard for full-field clinical electroretinography (2015 update). *Doc Ophthalmol*. 2015;130:1–12.
12. Lois N, Holder GE, Bunce C, Fitzke FW, Bird AC. Phenotypic subtypes of Stargardt macular dystrophy-fundus flavimaculatus. *Arch Ophthalmol*. 2001;119:359–369.
13. Robson AG, Webster AR, Michaelides M, et al. "Cone dystrophy with supernormal rod electroretinogram": a comprehensive genotype/phenotype study including fundus autofluorescence and extensive electrophysiology. *Retina*. 2010;30:51–62.
14. Neveu MM, Dangour A, Allen E, et al. Electroretinogram measures in a septuagenarian population. *Doc Ophthalmol*. 2011;123:75–81.
15. Holder GE, Robson AG. Paediatric electrophysiology: a practical approach. In: *Pediatric Ophthalmology, Neuro-Ophthalmology, Genetics*. Berlin: Springer-Verlag; 2006.
16. Cartegni L, Chew SL, Krainer AR. Listening to silence and understanding nonsense: exonic mutations that affect splicing. *Nat Rev Genet*. 2002;3:285–298.
17. Maugeri A, van Driel MA, van de Pol DJ, et al. The 2588G–>C mutation in the ABCR gene is a mild frequent founder mutation in the Western European population and allows the classification of ABCR mutations in patients with Stargardt disease. *Am J Hum Genet*. 1999;64:1024–1035.
18. Zernant J, Xie YA, Ayuso C, et al. Analysis of the ABCA4 genomic locus in Stargardt disease. *Hum Molec Genet*. 2014;23:6797–6806.
19. Webster AR, Heon E, Lotery AJ, et al. An analysis of allelic variation in the ABCA4 gene. *Invest Ophthalmol Vis Sci*. 2001;42:1179–1189.
20. Klevering BJ, Deutman AF, Maugeri A, Cremers FP, Hoyng CB. The spectrum of retinal phenotypes caused by mutations in the ABCA4 gene. *Graef Arch Clin Exp Ophthalmol*. 2005;243:90–100.
21. Sangermano R, Bax NM, Bauwens M, et al. Photoreceptor Progenitor mRNA analysis reveals exon skipping resulting from the ABCA4 c.5461-10T–>C mutation in Stargardt disease. *Ophthalmology*. 2016;123:1375–1385.
22. Rivera A, White K, Stohr H, et al. A comprehensive survey of sequence variation in the ABCA4 (ABCR) gene in Stargardt disease and age-related macular degeneration. *Am J Hum Genet*. 2000;67:800–813.
23. Zernant J, Schubert C, Im KM, et al. Analysis of the ABCA4 gene by next-generation sequencing. *Invest Ophthalmol Vis Sci*. 2011;52:8479–8487.
24. Littink KW, Koenekoop RK, van den Born LI, et al. Homozygosity mapping in patients with cone–rod dystrophy: novel mutations and clinical characterizations. *Invest Ophthalmol Vis Sci*. 2010;51:5943–5951.
25. Walia S, Fishman GA. Natural history of phenotypic changes in Stargardt macular dystrophy. *Ophthal Genet*. 2009;30:63–68.
26. Oh KT, Weleber RG, Oh DM, Billingslea AM, Rosenow J, Stone EM. Clinical phenotype as a prognostic factor in Stargardt disease. *Retina*. 2004;24:254–262.
27. Chen B, Tosha C, Gorin MB, Nusinowitz S. Analysis of autofluorescent retinal images and measurement of atrophic lesion growth in Stargardt disease. *Exp Eye Res*. 2010;91:143–152.
28. Fujinami K, Lois N, Mukherjee R, et al. A longitudinal study of Stargardt disease: quantitative assessment of fundus autofluorescence, progression, and genotype correlations. *Invest Ophthalmol Vis Sci*. 2013;54:8181–8190.
29. McBain VA, Townend J, Lois N. Progression of retinal pigment epithelial atrophy in stargardt disease. *Am J Ophthalmol*. 2012;154:146–154.
30. Zahid S, Jayasundera T, Rhoades W, et al. Clinical phenotypes and prognostic full-field electroretinographic findings in Stargardt disease. *Am J Ophthalmol*. 2013;155:465–473. e463.
31. Oh KT, Weleber RG, Stone EM, Oh DM, Rosenow J, Billingslea AM. Electroretinographic findings in patients with Stargardt disease and fundus flavimaculatus. *Retina*. 2004;24:920–928.
32. Fujinami K, Lois N, Davidson AE, et al. A longitudinal study of stargardt disease: clinical and electrophysiologic assessment, progression, and genotype correlations. *Am J Ophthalmol*. 2013;155:1075–1088.
33. Conley SM, Cai X, Makkia R, Wu Y, Sparrow JR, Naash MI. Increased cone sensitivity to ABCA4 deficiency provides insight into macular vision loss in Stargardt's dystrophy. *Biochim Biophys Acta*. 2012;1822:1169–1179.
34. Mullins RF, Kuehn MH, Radu RA, et al. Autosomal recessive retinitis pigmentosa due to ABCA4 mutations: clinical, pathologic, and molecular characterization. *Invest Ophthalmol Vis Sci*. 2012;53:1883–1894.
35. Caminsky N, Mucaki EJ, Rogan PK. Interpretation of mRNA splicing mutations in genetic disease: review of the literature and guidelines for information-theoretical analysis. *F1000Research*. 2014;3:282.
36. Cremers FP, van de Pol DJ, van Driel M, et al. Autosomal recessive retinitis pigmentosa and cone-rod dystrophy caused by splice site mutations in the Stargardt's disease gene ABCR. *Hum Molec Genet*. 1998;7:355–362.
37. Cideciyan AV, Swider M, Aleman TS, et al. ABCA4 disease progression and a proposed strategy for gene therapy. *Hum Molec Genet*. 2009;18:931–941.